

University of Nebraska - Lincoln

DigitalCommons@University of Nebraska - Lincoln

Ravi Saraf Publications

Chemical and Biomolecular Research Papers --
Faculty Authors Series

August 1995

Corrosion and Protection of a Conductive Silver Paste

V. Brusic

IBM Research Division, T.J. Watson Research Center, Yorktown Heights, New York

G. S. Frankel

IBM Research Division, T.J. Watson Research Center, Yorktown Heights, New York

J. Roldan

IBM Research Division, T.J. Watson Research Center, Yorktown Heights, New York

Ravi F. Saraf

University of Nebraska-Lincoln, rsaraf2@unl.edu

Follow this and additional works at: <https://digitalcommons.unl.edu/cbmesaraf>

 Part of the [Biomechanics and Biotransport Commons](#)

Brusic, V.; Frankel, G. S.; Roldan, J.; and Saraf, Ravi F., "Corrosion and Protection of a Conductive Silver Paste" (1995). *Ravi Saraf Publications*. 5.

<https://digitalcommons.unl.edu/cbmesaraf/5>

This Article is brought to you for free and open access by the Chemical and Biomolecular Research Papers -- Faculty Authors Series at DigitalCommons@University of Nebraska - Lincoln. It has been accepted for inclusion in Ravi Saraf Publications by an authorized administrator of DigitalCommons@University of Nebraska - Lincoln.

Corrosion and Protection of a Conductive Silver Paste

V. Brusica,* G. S. Frankel,* J. Roldan, and R. Saraf*

IBM Research Division, T.J. Watson Research Center, Yorktown Heights, New York 10598, USA

ABSTRACT

One of the possible uses for a conductive paste is as an adhesive in interconnect technology that could replace PbSn solder. The interconnections are expected to perform under a variety of environmental conditions, and with an applied voltage. Thus knowledge of their corrosion and dissolution resistance is of utmost importance. This is a study of the dissolution and protection of polymer/metal composite films, prepared with a high loading of silver or gold particles. Electrochemical tests were conducted in a droplet of triple-distilled water with or without benzotriazole (BTA) and BTA derivatives. Results indicate that, in spite of some protection obtained by the polymer, silver paste dissolution at high anodic potentials is rapid, reaching values of 10^{-1} A/cm², which corresponds to a catastrophic silver removal rate of at least 35.6 nm/s. With a reservoir of azole in the corrosive environment, this rate can be reduced by up to five orders of magnitude. This azole effect greatly reduces the probability of electrolytic silver migration, but the Ag dissolution rate is still higher than the anodic activity shown by Au paste under the same conditions.

Introduction

Insulating thermoset and thermoplastic polymers can be made conductive by loading them with metallic powder particles such as silver, copper, or gold. The resulting conductive paste has many potential applications. Such a material can be used for electrostatic discharge protection, electromagnetic interference shielding, and as adhesive for interconnect technology that could replace PbSn solder. The widespread use of Pb containing solder in electronics is an environmental concern, and regulations banning Pb are being considered. Whereas paste conductivity is the critical property in interconnection applications, the corrosion and dissolution resistance are also of the utmost importance. In order to be conductive, the paste has to have a high loading level, *i.e.*, it should contain more than 50 weight percent (w/o) of the metal powder. Interconnections are expected to perform under a variety of environmental conditions, and with an applied voltage, where metal dissolution can result in electrolytic migration, dendrite formation, and eventually electrical shorts or opens. Thus, the susceptibility of the paste to dissolve under an applied potential indicates a potential problem for a device in operation.

This is a study of the dissolution and protection of polymer/metal composite (PMC) films, prepared in our laboratory with a high loading of silver particles. Electrochemical tests were conducted in a droplet of triple-distilled water with or without benzotriazole (BTA) and BTA derivatives. Same of the patent literature,¹ as well as experience in our laboratory, has indicated that Ag forms a thin layer of Ag-BTA in a manner similar to Cu under the same conditions. Yet, the protective nature of Ag-BTA films is not well documented. Results are discussed in terms of observed protection offered by BTA and compared to the results obtained on a similar paste formulated with Au particles.

Experimental

The PMC samples were prepared on a glass substrate as blanket films with dimensions of 1.9×3.2 cm and a thickness range from 25 to 40 μm . Ag or Au particles (with a typical loading factor of 88 w/o) were used in the preparation of the paste. Some of the variations used in the PMC preparation include (i) additions of 1000 ppm BTA to the paste formulating mixture, (ii) 10 min immersion into an aqueous solution of 10^{-2} M BTA, and (iii) 3 min dip into an alcohol solution of BTA or 5CH₃BTA in concentrations of 0.02 and 0.2 M prior to electrochemical evaluation of the corrosion behavior in a selected electrolyte. The temperature of the alcohol-azole solution was controlled in the range of room temperature to 60°C.

Plating tape was used to expose an area of 0.32 cm² for electrochemical testing. The electrochemical cell also contained a Pt mesh as a counterelectrode and a mercurous sulfate electrode (MSE, with saturated solution of K₂SO₄) as a reference electrode, that were separated by a filter

* Electrochemical Society Active Member.

paper. This cell design, described elsewhere,² was proven suitable for use with a small volume of an electrolyte, 0.01 ml or so, and with electrolytes that are normally difficult to handle or have low conductivity. Because of the closeness of the electrodes, the cell is suitable for tests in water without significant ohmic potential drop. The use of pure water as an electrolyte mimics the conditions that apply in processing (such as product rinsing) or in exposure to a humid atmosphere. The electrochemical tests consisted of corrosion potential measurement, which was interrupted in regular time intervals by measurement of linear polarization to determine the corrosion rate. After about 10 min, when the open potential reached a stable value (changing no more than 2 mV/min), a potentiodynamic sweep was applied. A sweep rate of 1 mV/s was used, starting 250 mV below the corrosion potential and reaching 1.3 V *vs.* MSE. In several tests, dissolution of Ag paste was examined by an application of a constant anodic potential and a continuous recording of the current, *i.e.*, with potentiostatic control. The electrolyte was water, with or without BTA or an azole derivative.

Most of the electrochemical tests were conducted within hours of the paste preparation. Some of the experiments were performed after months of sample storage in either open containers, or in closed containers containing a dry 5CH₃-BTA reservoir.

In a few experiments, using Ag foil, ellipsometry was used to determine the presence and thickness of Ag-azole films on the silver surface, and time-of-flight static secondary ion mass spectroscopy (SIMS) was employed to determine the film composition.

Results and Discussion

Anodic dissolution of silver.—Although noble, silver dissolves in water saturated with air at a corrosion rate of

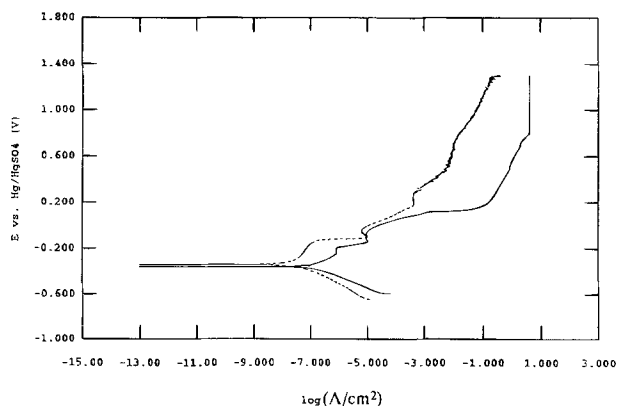


Fig. 1. Potentiodynamic polarization curves for an Ag foil (solid line) and Ag paste (dashed line) samples measured in a droplet of water.

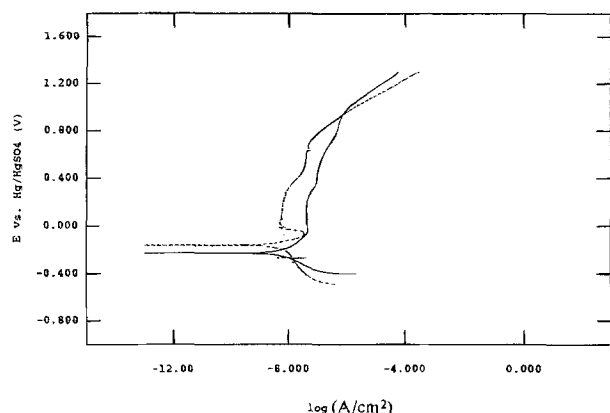


Fig. 2. Potentiodynamic polarization curves measured on Au film (solid line) and Au paste (dashed line).

about 1×10^{-7} A/cm² or 0.002 nm/min. The results obtained with a pure silver foil are shown in Fig. 1. With increased anodic potential, silver dissolution rapidly increases, in spite of the thermodynamic prediction of higher valent silver oxide formation.³ Apparently none of the oxides that are expected to form, Ag₂O, Ag₂O₂, and Ag₂O₃, are truly protective, and at high anodic potentials Ag dissolves with a current that (for the given experimental area) exceeds the measurable limit of the EG&G Princeton Applied Research 273 potentiostat. The highest measured current density of 10 A/cm² corresponds to the dissolution rate of 3.6×10^{-3} nm/s (with an assumption that at these anodic potentials Ag dissolves with a three-electron exchange). These very high anodic rates measured in water confirm what is already known from the anodic behavior of silver in aqueous solution⁴ and vast experience in electronic industry⁵: in the presence of humidity and bias, silver forms poorly passive, fairly soluble silver oxides. Dissolved ions increase the conductivity of the adsorbed water layers, easily migrate under the influence of the electric field, and provide reactants for the cathodic reaction, which is deposition of Ag dendrites. Thus the magnitude of the anodic current in the water droplet is a relative measure of the vulnerability to form electrical shorts in interconnection applications.

Metal coverage in the conductive paste.—The corrosion rate measured as current density (per geometric area) on Ag paste is about an order of magnitude smaller than that of Ag foil, Fig. 1. This indicates that the actual area of the metal available for reaction is about 10% of the available area, or that the polymeric coverage for this particular paste is about 90%.

Dissolution of Au paste.—In comparison to the Ag paste, the PMC film with Au particles has significantly lower currents both at the corrosion potential as well as at high anodic potentials, Fig. 2. As in the case of Ag, the apparent metal coverage in the paste is about 90%, judging from the dissolution rates at the corrosion potential. The Au paste is possibly contaminated with some Ag (from previous milling of the Ag paste during formulation) that could explain the observed current peak below 0 V. Both Au and Au paste show relatively low anodic currents below about 0.8 V. The measured current density of about 10^{-7} A/cm² is about an order of magnitude higher than the current due to charging of the double layer during the scan. For a double layer capacitance of 20 μ F/cm², the capacitive current would be approximately 2×10^{-8} A/cm². If the anodic current were caused by Au dissolution, an average Au removal rate would be 1.1×10^{-3} nm/s. The increase of the anodic current at potentials above 0.8 V is attributed to the evolution of oxygen, which proceeds much slower than does the dissolution of Ag at the same potentials.

Effect of BTA and 5CH₃BTA on dissolution of Ag.—Potentiodynamic curves measured in water with 10^{-2} M BTA

show remarkable reduction of the Ag dissolution rate, Fig. 3. An increase of the corrosion potential and a decrease of the corrosion rate suggest that the presence of this inhibitor slows down preferentially the anodic reaction in the overall corrosion process, similar to the reports for the effect of BTA on Cu corrosion.⁶ In contrast to the case of copper, however, BTA is even more effective at high anodic potentials, with the average dissolution rate being more than four orders of magnitude lower than that measured in water alone. Moreover, the anodic dissolution rate of Ag paste in the presence of BTA is almost as slow as the rate measured on pure Au paste.

Ellipsometric data on Ag foil that was immersed in the aqueous BTA solution, rinsed in water, and N₂ dried, show a formation of a surface film with a thickness of about 3 nm. This is very close to the thickness of Cu-BTA film that is normally formed on oxidized Cu surface under similar circumstance, *i.e.*, 2.5 nm,^{6,7} and thicker than the measured BTA films that weakly adsorb on metals, such as Fe, Ni, or Al, where the BTA film thickness is less than 0.5 nm. Time-of-flight static SIMS data indicate that the film is Ag-BTA. Ag⁺ ions most likely occupy the same site in the benzotriazole ring as the Cu⁺ ions in Cu-BTA complex. However, in contrast to Cu-BTA on Cu, thin Ag-BTA on Ag shows only a marginal protection against corrosion when retested for the corrosion in water without a BTA reservoir. At higher anodic potential, effects of the azoles were observed only when these inhibitors were present in a solution as a reservoir.

As the thermal instability of BTA and its derivatives is well documented,^{6,7} additions of BTA to the paste during fabrication were not expected to be successful in a preparation of a built-in azole reservoir. This was indeed confirmed by experiments. However, immersion of paste into an alcohol-azole solution resulted in a surface film that offered a significant protection in subsequent exposure to water, Fig. 3. Visual observation and ellipsometric investigation of the Ag foil immersed in an alcohol-azole solution and dried (without rinsing) show a presence of a thick, white film. After rinsing in alcohol, the foil retains its shine, and ellipsometry indicates the presence of a film that is about 3 nm thick. Thus, as well as forming a thin Ag-BTA complex, the process apparently blocks the pores in the paste by a precipitated, noncomplexed, azole.

The beneficial effect of the built-in azole reservoir increased with an increase in concentration and temperature of the azole-alcohol solutions. The most effective, reproducibly measured protection, was observed with concentrated azole solutions (0.2M or more) applied at 50 or 60°C for 3 min. Of the two azoles that were tested, 5CH₃BTA offered a more effective protection. In the best cases, such reservoirs decreased the anodic dissolution in water four

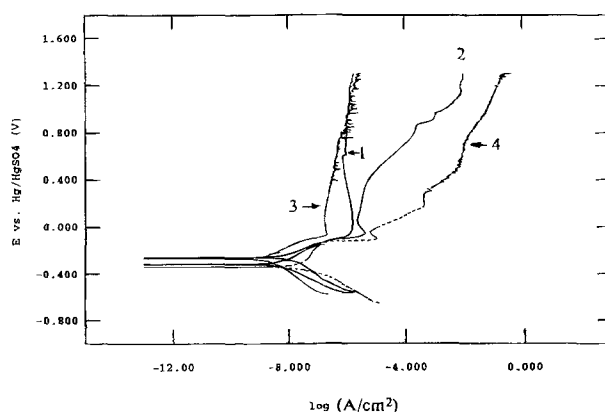


Fig. 3. Potentiodynamic polarization curves measured on Ag paste in aqueous solution of 0.01M BTA (1), and in triple distilled water (2 and 3) on Ag paste immersed for 3 min into an alcohol azole solution kept at 60°C prior to the measurements in water (2, alcohol contained 0.2M BTA; 3, alcohol contained 0.2M 5CH₃BTA alcohol). Data obtained on untreated Ag paste in water are plotted for a comparison (4).

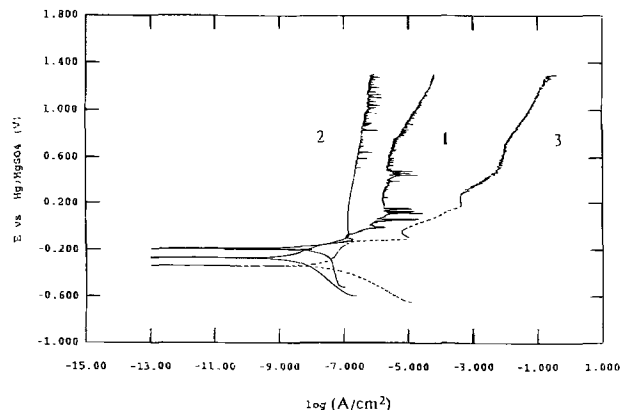


Fig. 4. Potentiodynamic curves measured on Ag paste treated with 5CH₃-BTA/alcohol mixture measured after 4 months of storage in an open container (curve 1). Results on unprotected paste (curve 3) and on protected paste, measured hours after the treatment (curve 2) are given for a comparison.

(with BTA) to five (for 5CH₃BTA) orders of magnitude. Under the best conditions, Ag dissolution approached the values measured on Au paste in water, with the Au paste still being better by an order of magnitude.

One of the most important properties of the paste, its electrical conductivity, is not changed by application of the azole reservoir. There are, however, some possible shortcomings of this treatment, such as its effects on the appearance and on the surface conductivity of the treated part. The altered surface appearance is a consequence of the azole application without rinsing, with a residual, nonuniform, film present over the entire exposed area. Its effect on surface conductivity cannot be easily predicted. By itself, this film is not conducting, and it should not cause electrical failures in the circuits. Dissolved in water, BTA increases solution conductivity: 0.01M BTA is 10 times more conductive than water alone. Thus, when the parts get exposed to an elevated relative humidity, dissolution of the azole in the adsorbed water layer should increase the conductivity of that film. The surface wetting, however, is expected to decrease for the azole-treated surface.⁸ The overall effect of the azole film on the behavior of an electronic circuit exposed to humidity and bias will be experimentally evaluated at a future time.

The potentiodynamic curves recorded on samples that were treated with the azole-alcohol solutions show some level of current instability (Fig. 3-5). The origin of the recorded noise is not fully understood, but it might be rooted in somewhat dynamic wetting of the rough paste surface, a fast localized dissolution of Ag, and a delayed

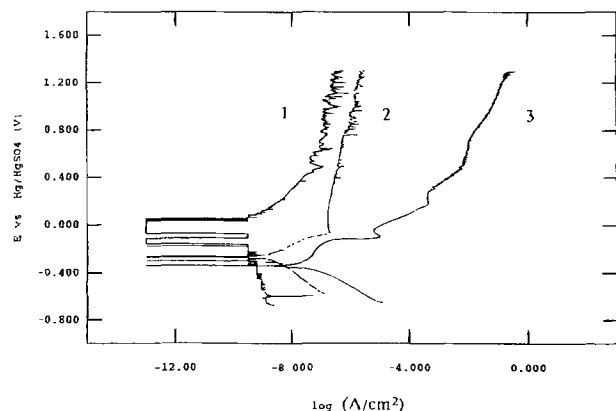


Fig. 5. Potentiodynamic curves measured on Ag paste treated with CH₃-BTA/alcohol mixture measured after 4 months of storage in a closed container with a surplus of CH₃-BTA powder (curve 1). Results on unprotected paste (curve 3) and on protected paste, measured hours after the treatment (curve 2) are given for a comparison.

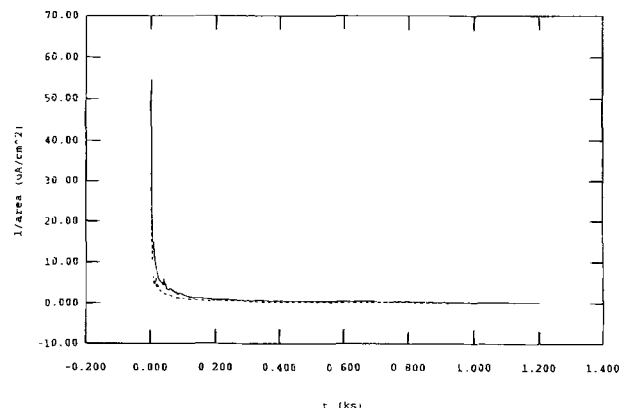


Fig. 6. Variation of current density with time during potentiostatic oxidation of azole-alcohol treated paste at 0.5 V (dashed line) and 1.0 V MSE (solid line) in water. Sample was stored in an azole containing container for 6 months prior to the electrochemical test.

reaction of Ag ions with dissolved azole. In contrast, anodic currents obtained on azole-alcohol treated samples in potentiostatic experiments are very stable. Figure 6 shows the current density-time curves for a sample treated with 5CH₃-BTA and stored in a closed container with a surplus of azole for more than 6 months and then oxidized in water at 0.5 and 1.0 V MSE, respectively, for 20 min. Similar data for untreated paste oxidized at 0.15 V are shown in Fig. 7. The steady-state current densities follow closely the behavior predicted from the potentiodynamic polarization curves, Fig. 1 and 5. Oxidation of Ag is fast, causing noticeable surface roughening, dissolution and precipitation of silver oxides, all resulting in a large variation in current density. Dissolution rate is of the order of magnitude of 0.15 A/cm² at 0.15 V, Fig. 7. (In comparison, currents obtained on Ag foil are higher and even more noisy.) The azole-alcohol treated sample shows a dissolution rate below 1 × 10⁻⁸ A/cm² at 0.15 V, 3.7 × 10⁻⁸ A/cm² at 0.5 V, and 3.1 × 10⁻⁷ A/cm² at 1.0 V. Thus, again, the reduction of the dissolution rate provided by the azole-alcohol treatment is at least five orders of magnitude.

Both BTA and 5CH₃-BTA have relatively high vapor pressure (0.09 and 0.02 mm Hg at 40°C, respectively), and the paste protection by noncomplexed azoles should decrease with time. Thus the electrochemical tests were repeated four months after the application of the 5CH₃-BTA/alcohol treatment with some films being stored in an open container and some in a closed container that also had an added CH₃-BTA powder. The results are given in Fig. 4 and 5. Sample stored in an open container has somewhat higher corrosion rate as well as a dissolution rate at higher anodic potentials than measured immediately after CH₃-BTA application, but the dissolution is still about four orders of

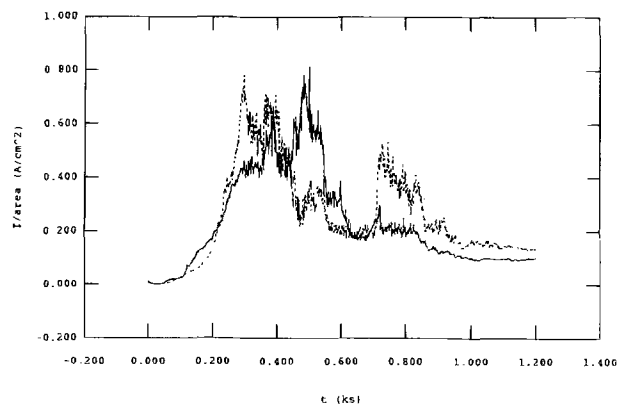


Fig. 7. Variation of current density with time during potentiostatic oxidation of untreated Ag paste at 0.15 V. Results of two separate experiments are plotted.

magnitude slower than that measured on unprotected paste, Fig. 4. A sample stored in a closed container with a reservoir of $\text{CH}_3\text{-BTA}$ powder has improved its corrosion and dissolution resistance, and its overall activity is smaller than measured on Au paste, Fig. 5.

Conclusions

1. The polymer used in the paste fabrication provides coverage of more than 90% for Ag particles, and a corresponding decrease of the Ag corrosion and dissolution. In spite of the protection, the dissolution of silver at anodic potentials reaches the current density of 10^{-1} A/cm², which far exceeds the rate of oxygen evolution and corresponds to the rate of Ag removal of at least 35.6 nm/s.

2. In an aqueous solution containing BTA, the anodic dissolution of Ag particles is greatly reduced. The behavior of the paste becomes similar to that of Au paste except for the fact that even the oxygen evolution reaction is greatly suppressed.

3. A reservoir with either BTA or $5\text{CH}_3\text{BTA}$ can be built into the paste by a short immersion of the paste into an alcohol-azole mixture at elevated temperature followed by nitrogen drying. The bulk of the residual film is composed of noncomplexed BTA or $5\text{CH}_3\text{BTA}$. Because of their relatively high vapor pressure, (0.09 mm Hg for BTA and 0.02 mm Hg for $5\text{CH}_3\text{BTA}$), these films should disappear with time. $5\text{CH}_3\text{BTA}$ is both a better protector and more stable than BTA. The effective protection of either of these

films can be prolonged indefinitely, if they are kept in an enclosure with a solid azole reservoir.

Manuscript submitted Jan. 30, 1995; revised manuscript received April 7, 1995. This was Paper 223 presented at the Miami Beach, FL, Meeting of the Society, Oct. 9-14, 1994.

IBM Research Division assisted in meeting the publication costs of this article.

REFERENCES

1. S. Kobayashi, M. Itoh, and A. Minato, U. S. Pat. 4,821,148 (1989).
2. V. Brusic, M. Russak, R. Schad, G. Frankel, A. Selius, D. DiMilia, and D. Edmonson, *This Journal*, **136**, 42 (1989).
3. M. Pourbaix, *Atlas of Electrochemical Equilibria*, Pergamon Press, New York (1966).
4. U. Ebersbach, K. Schwabe, and K. Ritter, *Electrochim. Acta*, **12**, 927 (1967).
5. J. J. Steppan, J. A. Roth, L. C. Hall, D. A. Jeannotte, and S. P. Carbone, *This Journal*, **134**, 175 (1987).
6. V. Brusic, M. A. Frisch, B. N. Eldridge, F. P. Novak, F. B. Kaufman, B. M. Rush, and G. S. Frankel, *ibid.*, **138**, 2253 (1991).
7. V. Brusic, M. A. Frisch, B. N. Eldridge, F. B. Kaufman, T. A. Petersen, A. Schrott, and G. S. Frankel, in *Proceedings of International Symposium on Control of Copper and Copper Alloys Oxidation*, Edition de la Revue de metallurgy, Paris (1993).
8. R. R. Thomas, V. A. Brusic, and B. M. Rush, *This Journal*, **139**, 678 (1992).

Rupture of an Oxide Blister

R. L. Ryan and E. McCafferty

Naval Research Laboratory, Washington, DC 20375, USA

ABSTRACT

Expressions have been derived which describe the critical stress and pressure necessary to rupture oxide blisters which form on aluminum during the growth of corrosion pits. These expressions have been derived and evaluated for radial cracks in the oxide blister. The critical stress and corresponding pressure for rupture decrease with increasing blister radius and decrease with increasing crack length. The critical stress is independent of the ratio of oxide film thickness to blister radius, whereas the rupture pressure increases with this ratio. The critical stress is independent of Poisson's ratio for the oxide film whereas the rupture pressure is weakly dependent on Poisson's ratio for the oxide film.

Introduction

The propagation of corrosion pits on aluminum leads to the formation and rupture of blisters above the corrosion pit.¹⁻⁵ These blisters are produced by the generation of hydrogen gas within the active pit. A previous detailed study¹ has shown that such blisters evolve through four stages: (i) the formation of a primary crack or pore in the oxide film (see Fig. 1) so as to allow contact between the solution and underlying metal, (ii) metal dissolution and hydrogen production at the oxide/metal interface, (iii) formation of a hydrogen pocket within the blister, and (iv) eventual rupture of the blister caused by the increasing hydrogen pressure (see Fig. 2).

As has been noted previously,¹ the hydrogen bubble will stay trapped under a cracked film because small bubbles are unstable and will grow into a larger bubble. For a spherical bubble of radius r , the pressure differential p across the bubble is given by the well-known Young and Laplace equation: $p = 2\gamma/r$, where γ is the surface tension of the membrane. The pressure differential is greater for small values of r so that this internal pressure will cause the bubble to grow into a bubble of larger r . Pickering and Harris^{6,7} have provided evidence for the formation of large stable bubbles within localized corrosion cells.

In Ref. 1, the critical stress associated with blister rupture was calculated via a Griffith-type analysis. That anal-

ysis was based on the *a priori* assumption of a hemispherical blister. Also, the rupture pressure was not explicitly calculated. In the present analysis, calculations of both the rupture stress and rupture pressure, based on the equilibrium shape of the blister, are provided for radial cracks in a blister as shown in Fig. 1.¹

Equilibrium Shape of a Blister

From the data given in Ref. 1, it is apparent that the thickness-to-radius ratio, $S = h/a$, is of the order 10^{-3} , whereas the peak vertical displacement of the pressurized blister is much greater than h . Accordingly, the blister may be modeled as a very thin membrane with no flexural resistance and undergoing large deflection. A close approximation to the deformed shape of the blister, as well as the membrane stresses, can be obtained by the principle of virtual displacements.⁸ It is assumed that the membrane is fixed to the base metal along a circular perimeter, and the internal pressure is constant. Thus, prior to the rupture process, the deformed shape has circular symmetry. The strain energy of the membrane, expressed in polar coordinates is⁸

$$V = \frac{1}{2} \int_A \int_A (N_r \epsilon_r + N_\theta \epsilon_\theta) r dr d\theta \quad [1]$$